Chapter 5
Metal Organic Frameworks

5.1 Introduction

Metal organic frameworks (MOF) are hybrid materials, based on transition metal ions and organic linker components (Kitagwa *et al*., 2004, Mueller *et al*., 2006). Linker components are made up of an organic molecule which contains some sort of functionality at its terminal positions. Functionality amongst linkers may vary, but the two most common groups that are currently being utilised for MOF production are pyridyls and carboxylates. Functionality of the linker components is vital for MOF production as they allow the organic linker to join the metals by coordinating to them through the functional groups. A key feature of these materials is the relative ease with which framework topology can be altered. This is achieved by utilising various metal and linker components, resulting in the formation of 1D, 2D and 3D network structures (Janiak, 2003). Alteration thus, allows these materials to be fine tuned to suit specific applications. In this project we obtained four new MOF structures using the gly-L linker (ligand) with three divalent metals. The structures obtained are discussed and compared in this chapter.

5.2 Synthesis

MOF-Zn1 was obtained by using a 3:1 ligand (gly-L) to metal ($ZnNO_3$. $6H_2O$) ratio containing 3 drops of H_2O_2 (hydrogen peroxide) and 3 drops dichlorobenzene (as blocking agent) in a 5ml dimethylformamide (DMF) solution in accordance to a similar synthesis by Li *et al*. (1999). This solution was then placed into a larger vial containing toluene (5ml) and 3 drops of triethylamine, and vapour diffusion was allowed to take place at room temperature.

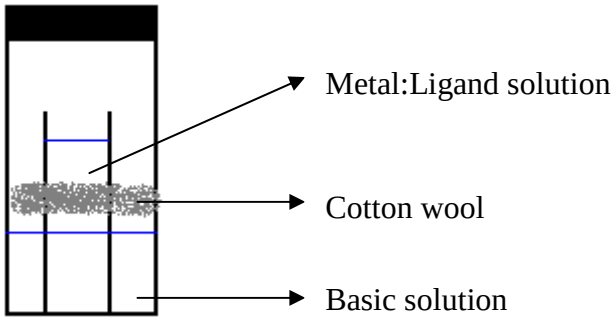

Figure 5.1: Vapour diffusion setup.

MOF-Zn2, MOF-Cd1 and MOF-Co1, were all synthesised in exactly the same manner as MOF-Zn1. The only difference in one case was that MOF-Co1 was placed in a fridge to facilitate crystal growth.

5.3 Crystal morphology

Images of the various MOF crystal forms were obtained using an Olympus SZ60 microscope at 50x magnification. This allowed for the examination of the crystal morphology of materials grown from the different metals, figure 5.2.

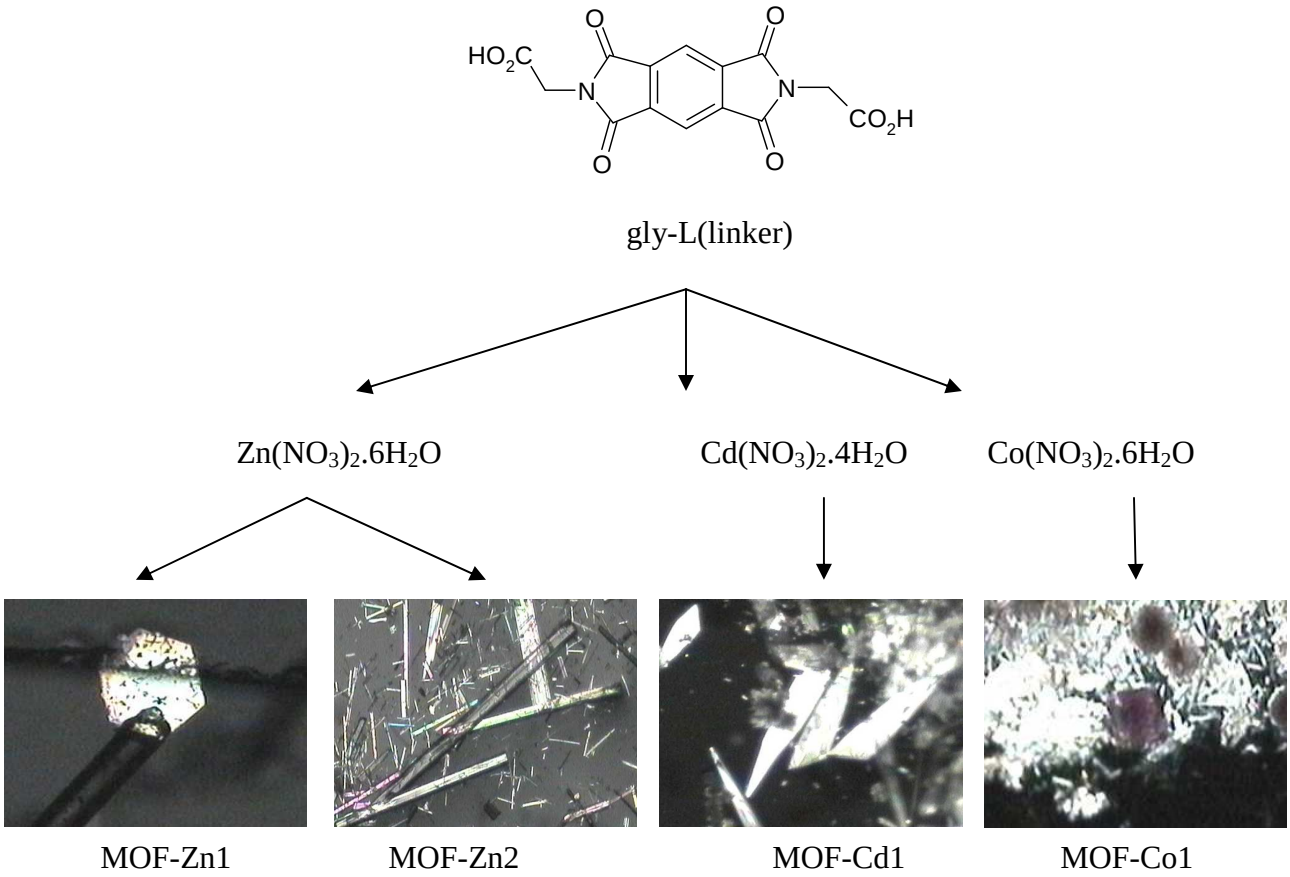

Figure 5.2: Optical microscope images at 50x magnification of the various MOFs grown using various divalent metals with gly-L.

Figure 5.2, indicates noticeable differences in crystal morphology amongst all three metals. The usage of zinc metal led to the formation of two different crystal morphologies i.e. plates and needles from one synthesis. Cadmium nitrate formed large prismic blocks, whilst the use of cobalt nitrate produced tiny pink fragile blocks that were difficult to manipulate.

All MOF structures showed similar stability in air once removed from the mother liquor. The approximate decomposition time of all crystals was found to be less than a minute. Due to the poor stability of these materials in air, crystals were placed in oil and were assessed using SCXRD. Once the correct crystal was obtained it was

mounted onto the goniometer head containing a copper mount and data was collected at -100^{o}C.

5.4 Single Crystal X-Ray Diffraction

The four new MOF materials were successfully characterised via SCXRD, and each structure is discussed with regard to metal coordination and crystal packing.

The relevant crystallographic data for the MOF structures synthesised in this work are given in table 5.1. SCXRD confirms the formation of two different structures for MOF-Zn as indicated by optical microscopy. The table below indicates that MOF-Zn1 contains has the highest crystallographic symmetry of all MOFs crystallising in orthorhombic *Pbca,* followed by a monoclinic $P2_1/c$ crystal system for MOF-Co1. Both MOF-Zn2 and MOF-Cd1 crystallised in triclinic *P*-1 system. Unit cell volumes varied tremendously between MOFs, with MOF-Zn1 containing the largest cell volume of 5345Å^3 with 8 formula units, followed by MOF-Zn2 with 4754Å^3 containing 2 formula units, then MOF-Co1 with 2758Å^3, and 4 formula units and lastly by MOF-Cd1 with 580Å^3, and 2 formula units.

With the exception of MOF-Zn2, all MOF contain two coordinated DMF solvent molecules in the apical position of the coordination environment. MOF-Zn1, Co1 and Zn2 each contain a single uncoordinated DMF molecule within the asymmetric unit cell with MOF-Zn2 containing 4 additional triethylamine uncoordinated solvent molecules.

Table 5.1: Crystallographic data for the MOFs reported in this chapter.

Crystal	**MOF-Zn1**	**MOF-Zn2**	**MOF-Cd1**	**MOF-Co1**
Emperical formula	C_{23} H_{27} N_5 O_{11} Zn	C_{43} H_{51} N_7 O_{17} Zn	C_{20} H_{20} N_4 O_{10} Cd	C_{23} H_{29} N_5 O_{12} Co
$M_{r\ (g.mol^{-1})}$	614.9	1003.3	588.8	624.4
Temperature/K	173 (2)	173 (2)	173 (2)	173 (2)
Cell setting	Orthorhombic	Triclinic	Triclinic	Monoclinic
Space group	*Pbca*	*P*-1	*P*-1	$P2_1/c$
a/Å	21.127(32)	11.457(1)	4.9774(10)	15.358(6)
b/Å	8.929(10)	16.302(3)	9.106(2)	18.861(6)
c/Å	28.337(36)	27.137(4)	12.849(2)	9.811(4)
α/°	90.000	74.392(1)	91.198(10)	90.000
β/°	90.000	80.846(1)	92.145(10)	103.889(2)
γ/°	90.000	85.840(1)	94.382(10)	90.000
V/Å^3	5345.33(12)	4817.20(16)	580.11(5)	2758.79(18)
Z, D_{calc}/g cm^{-3}	8, 1.53	2, 1.380	2, 1.685	4, 1.510
μ/mm^{-1}, F(000)	0.987, 2543.5	0.588, 2096	1.004, 296	0.693, 1300
Crystal size/mm	0.10 × 0.14 × 0.47	0.55 × 0.09 × 0.07	0.55 × 0.10 × 0.08	0.19 × 0.14 × 0.06
Absorption correction	None	None	None	None
θ_{max}/°	28.30	28.00	28.00	26.00
h, *k*, *l* (min, max)	(-27, 28), (-11, 11), (-37, 35)	(-15, 15), (-21, 21), (-35, 35)	(-6, 6), (-11, 11), (-16, 16)	(-18, 18), (-23, 23), (-12, 12)
Reflections collected	41283	85216	12820	17488
Unique reflections	6618	23213	2795	5409
Observed reflections	4560	14425	2748	2970
No. of parameters	361	1122	180	378
R_{int}	0.0812	0.0492	0.0580	0.0986
R_1 , wR_2	0.113, 0.261	0.047, 0.140	0.030, 0.076	0.063, 0.140
R_1, Wr_2 (all data)	0.143, 0.271	0.072, 0.148	0.030, 0.077	0.138, 0.180
GoF	1.114	0.967	1.074	0.999
$\Delta\rho_{max}$, $\Delta\rho_{min}$ (eÅ^{-3})	0.764, -1.091	0.794, -0.325	1.794, -0.563	0.932, -0.710

5.5 Crystal Structure Analysis

5.5.1 MOF-Zn1

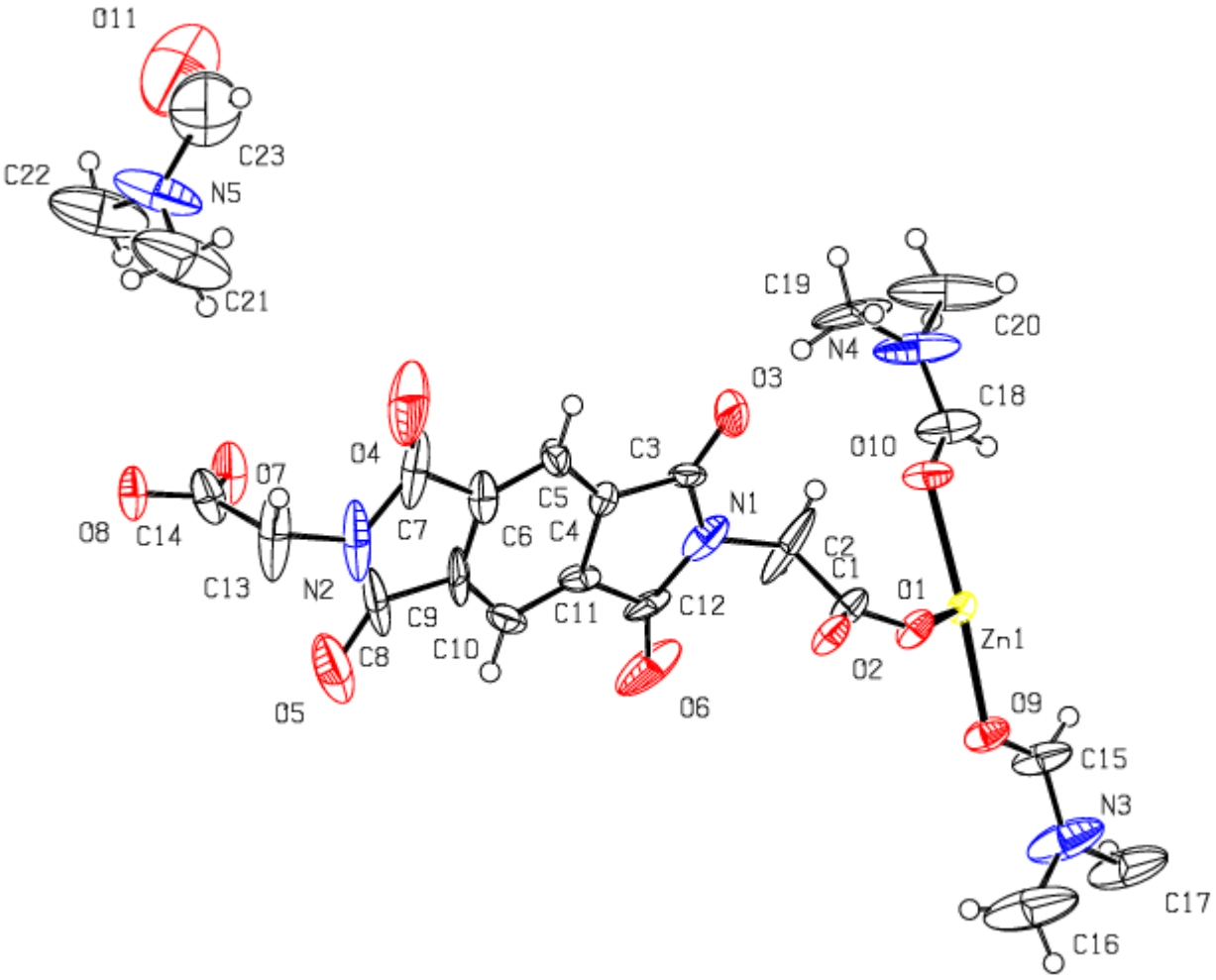

Figure 5.3: Ortep diagram of MOF-Zn1 drawn at the 50% probability level.

5.5.1.1 Metal coordination

Metal coordination of the ligand is vital in the formation of Metal Organic Frameworks. The coordination is responsible for the MOF topology, as it gives the material its overall structure which can be exploited for various applications.

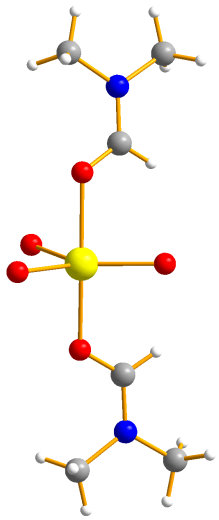

Figure 5.4: Coordination environment adopted by MOF-Zn1.

Figure 5.4 illustrates the trigonal bipyramidal coordination environment adopted in the structure of MOF-Zn1. Two DMF molecules occupy the apical positions whilst gly-L linker molecules coordinated to the equatorial plane. Each carboxylate group associated with the gly-L molecule attaches differently to the zinc metal. One gly-L carboxylate coordinates in a bidentate fashion as a consequence acting as a bridging ligand between the Zn atoms (∟O1-Zn-O2, 99.15^{o}). Whereas the other carboxylate coordinates to the metal in a monodentate fashion. The bridging caboxylate is essential for 2D extension of the structure resulting in Zn···O coordinated chains. These chains are linked to each other through the ligands resulting in the 2D layers shown in figure 5.5. The DMF molecules on each adjacent zinc metal are arranged in an offset manner relative to each other with a torsion angle of 59.08^{o} (O10-Zn1-Zn1-O9) within the 2D layers.

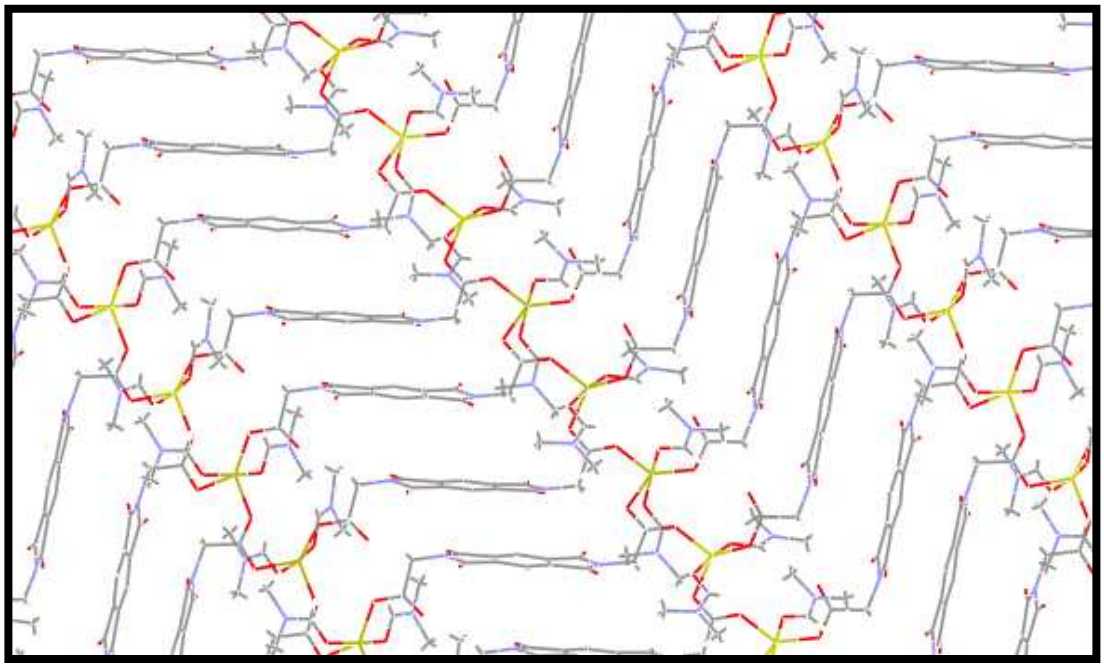

Figure 5.5: Two dimensional structural extension of MOF-Zn1 indicating a herringbone type arrangement.

5.5.1.2 3D structure

Figure 5.5 indicates that the *trans* orientation of the carboxylate groups associated with the ligand is maintained when coordinated to the metal. This results in the formation of 'zig-zag' like 2D layers and hence a herringbone type overall structure. The planar components associated with gly-L are aligned in a parallel manner relative to each other, and do not directly overlap each other. Instead they are off-set by an angle of 118.48° (C10-H10-H5) with a *Cg*···*Cg* inter-planar distance of 3.308Å.

The bridging ligand is responsible for the 2D layer formation, which is further stabilised through hydrogen bonding via the various IC and GC carbonyl groups with the apical DMF molecules. Three dimensional extension occurs by means of weak intermolecular hydrogen bonding between the DMF (apical and solvent) with the IC carbonyl atoms O4 and O5, and the C10 aromatic hydrogen (ArH). These interactions are tabulated below.

Table 5.2: CH···O hydrogen bond extension for MOF-Zn1.

Molecular interaction	Interaction	D—H/Å	H···A/Å	D···A/Å	∟D—H···A/°
DMF---GC (2D)	C15—H···O7	0.930	2.412	3.342(20)	154.68(70)
DMF---IC (2D)	C17—Hb···O5	0.960	2.447	3.407(30)	142.24(90)
DMF---IC (2D)	C19—Hc···O6	0.960	2.391	3.351(20)	143.37(90)
DMF---IC (3D)	C16—Ha···O4	0.961	2.625	3.586(30)	135.33(100)
ArH---DMF solv (3D)	C10—H···O11	0.930	2.541	3.471(30)	170.46(80)
DMF solv---IC (3D)	C23—H···O5	0.927	2.668	3.595(40)	160.99(200)

Pores in MOF-Zn1 are only evident once the solvent molecules are removed as represented in the figure 5.6. However it should be kept in mind that the removal of the solvent DMF molecules will lead to the collapse of the structure as it is essential for extension as well as stabilisation.

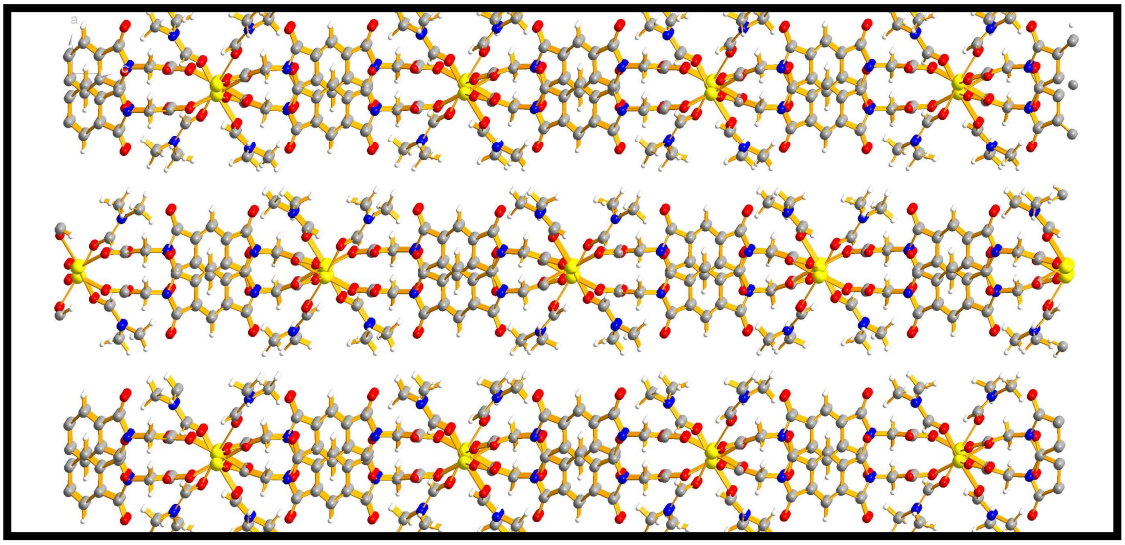

Figure 5.6: Pores visible upon removal of DMF solvent molecules, viewed along the *b*-axis.

5.5.2 MOF-Zn2

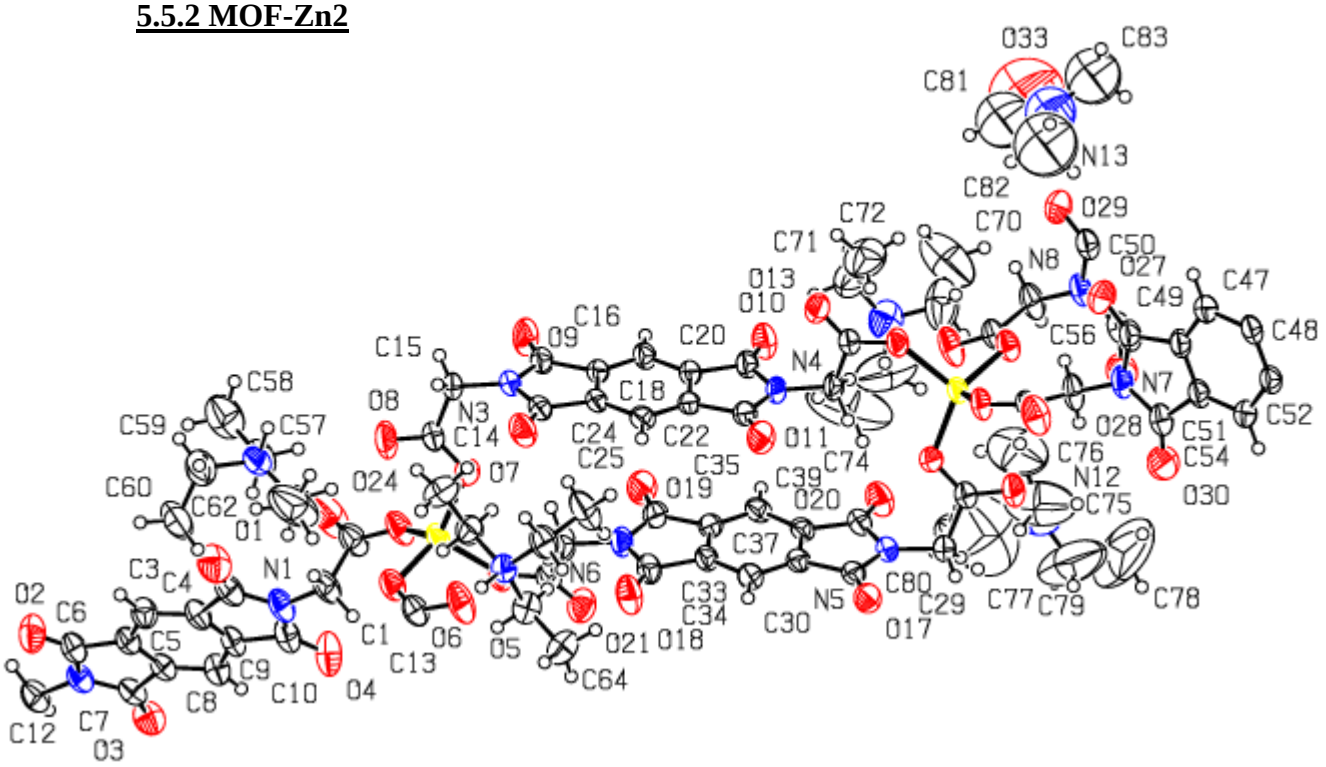

Figure 5.7: Ortep diagram of MOF-Zn2 drawn at the 50 % probability level.

5.5.2.1 Metal Coordination

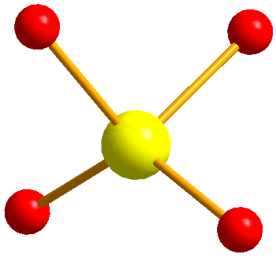

Figure 5.8: Tetrahedral coordination environment adopted by MOF-Zn2.

The above figure illustrates the tetrahedral coordination environment adopted by MOF-Zn2. The zinc metal coordinates to four different gly-L molecules in a monodentate fashion. Unlike MOF-Zn1, MOF-Zn2 does not contain any solvent molecules within its coordination environment. The resulting coordination geometry

of the metal and linker allows for the formation of 1D chains in which two gly-L linker components are stacked on top of each other, as indicated below.

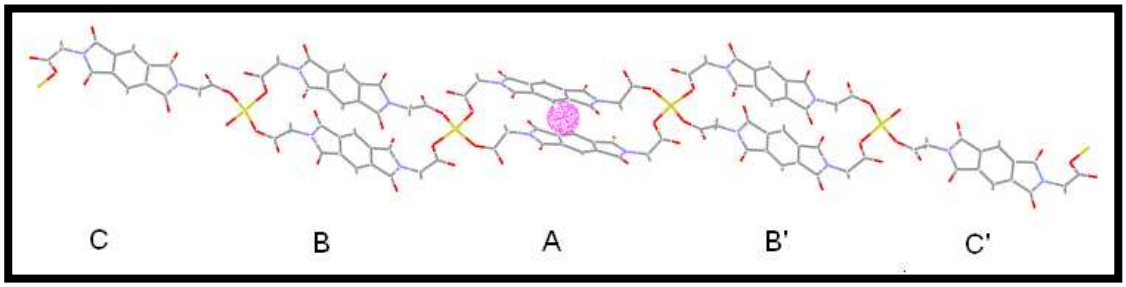

Figure 5.9: Coordination geometry leading to one dimensional chains, with stacking of aromatic ligands, and pink sphere indicating centre of inversion.

5.5.2.2 3D structure

MOF-Zn2 is made up of centrosymmetric 1D chains, which contains a centre of inversion between the planar components of the gly-L ligand (figure 5.9). The structure is broken down into three parts, namely A, B and C, for simplicity. Each part of the structure is made up of a pair of gly-L ligands that are offset relative to each other. The pair of ligand molecules associated with part A of the structure are offset by an angle of 82.26° (C9-H9-H4) with an inter-planar distance of 3.422Å, whilst those in part B are offset by 68.59° (C18-H18-H37) and a distance of 3.487Å, and those in part C offset by an angle of 108.69° (C47-H47-H52) and a distance of 3.569Å.

These 1D chains further extend into 2D layers through weak intermolecular hydrogen bonding between the various IC and GC carbonyl groups with the alkyl CH_2 and ArH (associated with gly-L ligand). The extension into 3D structures occurs through interactions between the guest triethylamine (TEA) molecules and the IC and GC carbonyl groups. The various weak hydrogen bonding interactions responsible for the 2D and 3D extension of the structure amongst all three parts (A, B, and C) are tabulated below.

Table 5.3: CH···O hydrogen bond interactions in MOF-Zn2.

Molecular interaction	Interaction	D—H/Å	H···A/Å	D···A/Å	∟D—H···A/°
Part A					
CH_2---GC (2D)	C12—Ha···O26	0.992	2.435	3.427(5)	153.11(20)
TEA---IC (3D)	C57—Hb···O1	0.990	2.680	3.670(5)	158.20(20)
TEA---IC (3D)	C61—Hb···O3	0.990	2.500	3.490(6)	148.03(20)
TEA---GC (3D)	C63—Hb···O5	0.991	2.533	3.524(5)	123.88(20)
TEA---GC (3D)	C76—Hc···O24	0.978	2.527	3.505(9)	130.22(30)
TEA---GC(3D)	C78—Ha···O5	0.979	2.532	3.511(10)	174.58(60)
Part B					
CH_2---GC (2D)	C15—Hb···O13	0.990	2.357	3.347(5)	148.75(20)
ArH---IC (2D)	C18—H ···O17	0.949	2.336	3.285(4)	162.99(10)
ArH---IC (2D)	C32—H ···O9	0.950	2.467	3.417(4)	164.54(10)
TEA---GC (3D)	C57—Ha···O8	0.989	2.243	3.232(5)	167.65(20)
TEA---GC (3D)	C62—Ha···O13	0.980	2.659	3.639(7)	131.05(30)
TEA---IC (3D)	C63—Ha···O18	0.989	2.539	3.528(5)	143.47(20)
TEA---IC (3D	C65—Ha···O11	0.990	2.670	3.660(5)	144.95(20)
TEA---IC (3D)	C65—Hb···O17	0.990	2.531	3.521(5)	137.17(40)
TEA---IC (3D)	C66—Hc···O12	0.980	2.647	3.627(5)	160.27(20)
TEA---IC (3D)	C67—Ha···O12	0.990	2.376	3.366(5)	152.28(20)
TEA---IC (3D)	C74—Hb···O20	0.981	2.677	3.658(9)	139.01(50)
TEA---GC (3D)	C77—Ha···O21	0.990	2.702	3.692(10)	159.83(60)
Part C					
ArH---IC (2D)	C52—H···O29	0.950	2.422	3.372(4)	167.44(20)
CH_2---IC (2D)	C56—Ha···O4	0.990	2.506	3.496(5)	133.03(20)
TEA---IC (3D)	C59—Hb···O29	0.990	2.675	3.665(5)	129.87(20)
TEA---GC (3D)	C67—Hb···O26	0.990	2.636	3.626(4)	122.14(20)
TEA---GC (3D)	C73—Hb···O32	0.991	2.563	3.554(7)	137.69(30)

The resulting extension of MOF-Zn2 through weak intermolecular hydrogen bonding, results in the formation of empty 1D channels with a pore diameter of 56Å^3 (PLATON) in alternating layers down the *a*-axis.

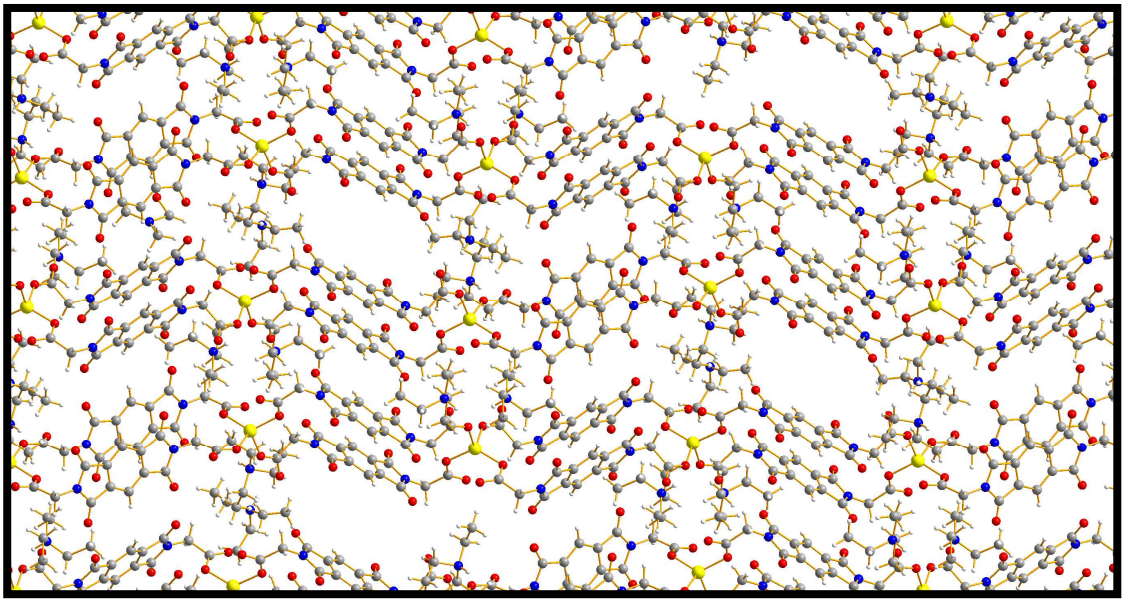

Figure 5.10: 1D pores in the structure of MOF-Zn2 viewed down the *a*-axis.

5.5.3 Metal coordination of MOF-Cd1

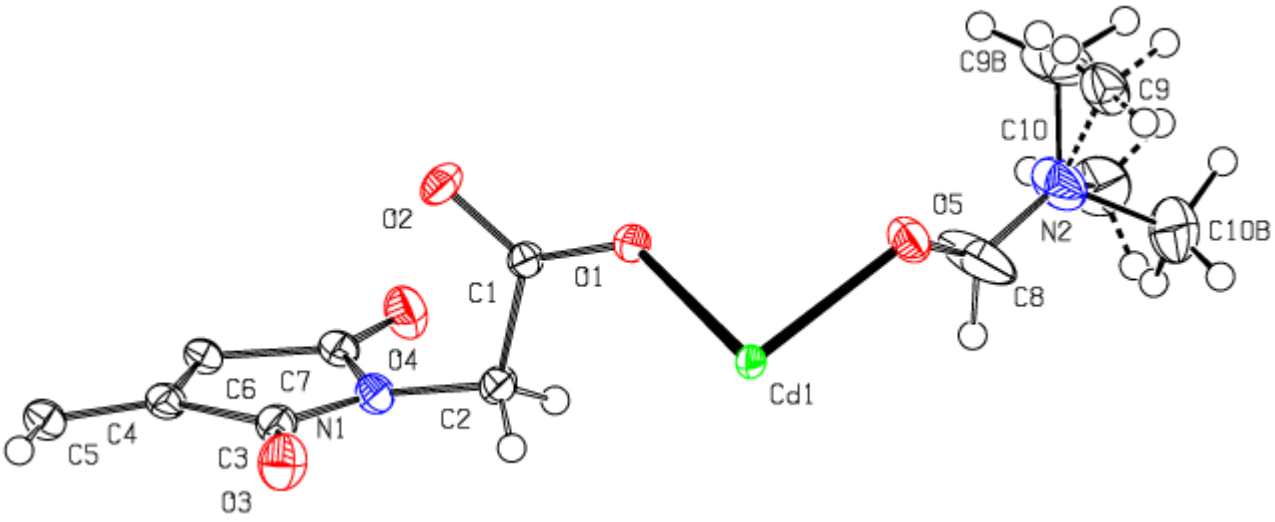

Figure 5.11 Ortep diagram of MOF-Cd1 at 50% probabilty level, showing the resolved disordered apical DMF molecules.

5.5.3.1 Metal Coordination

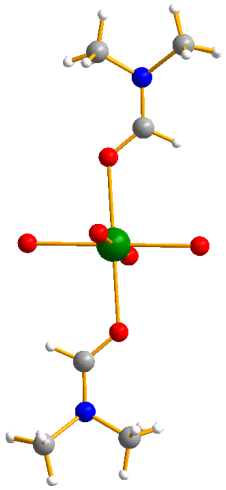

Figure 5.12: Octahedral coordination environment adopted by MOF-Cd1.

MOF-Cd1 adopts a symmetrical octahedral coordination environment, due to the cadmium metal occupying a centre of inversion. The DMF molecules occupy the

apical sites, whilst the carboxylates of the gly-L ligand coordinate to the metal in a bridging bidentate fashion with an angle of 91.36^{o} (O1-Cd-O2). The DMF molecules associated with the coordination environment are inverted relative to one another.

.

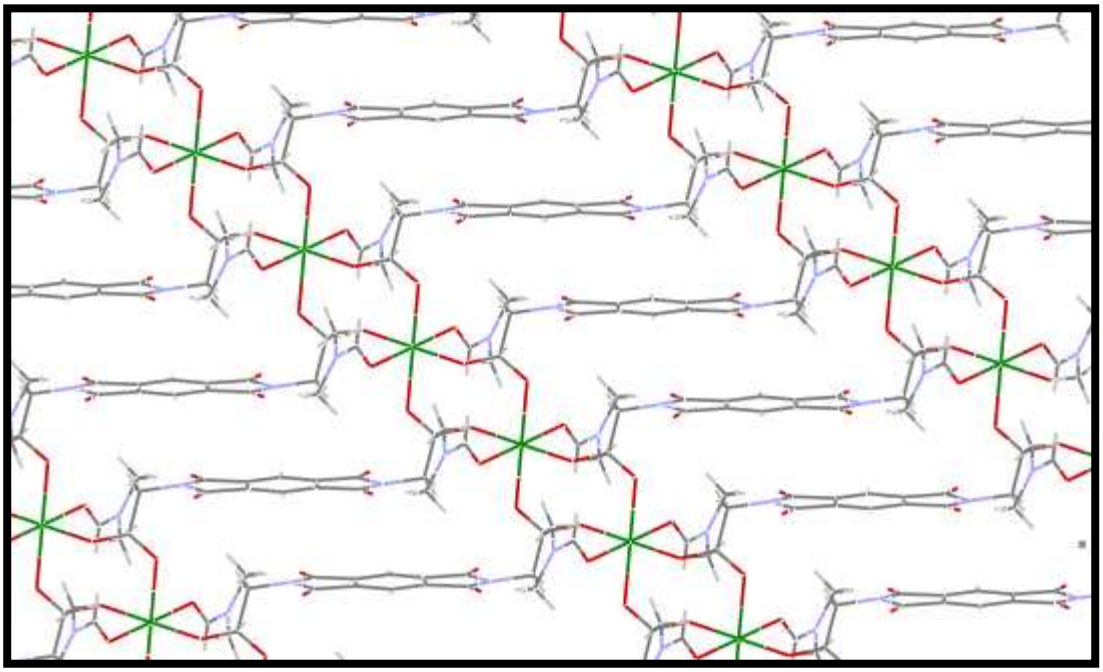

Figure 5.13: Two dimensional extension of MOF-Cd1, resulting in step-like arrangement.

5.5.3.2 3D structure

The bridging bidentate coordination of the gly-L ligand, coupled with the ligand geometry enables the MOF structure to extend in a step-like arrangement forming 2D sheets, figure 5.13. The planar rings are offset relative to one another by an angle of 90.83° (C5-H5-H5), with an inter-planar distance of 3.379Å, but are parallel. Unlike the other structures obtained, MOF-Cd1 does not contain any uncoordinated solvent molecules within its unit cell. It therefore extends into the third dimension due to weak intermolecular hydrogen bonding through the O3 and O4 IC planar carbonyl groups with the apical DMF molecules, table 5.4.

Table 5.4: CH···O hydrogen bond extension of MOF-Cd1.

Molecular interaction	Interaction	D—H/Å	H···A/Å	D···A/Å	∟D—H···A/°
DMF---IC (3D)	C9—Hb···O3	0.980	2.683	3.663(11)	149.17(50)
DMF---IC (3D)	C9—Hc···O3	0.980	2.176	3.156(10)	157.22(50)
DMF---IC (3D)	C9—Ha···O4	0.980	2.902	3.882(9)	122.78(50)

This hydrogen bonding allows the formation of very small 1D channels along the *a*-axis, containing a pore diameter of 29Å^3 (PLATON).

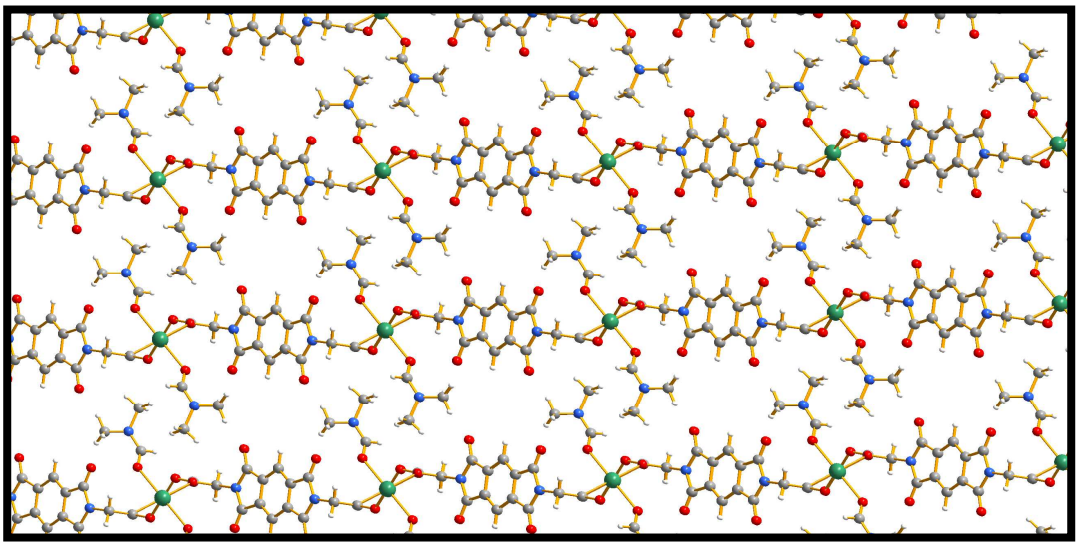

Figure 5.14: Illustration of 1D open network pores along the *a*-axis in the structure of MOF-Cd1.

5.5.4 Metal coordination of MOF-Co1

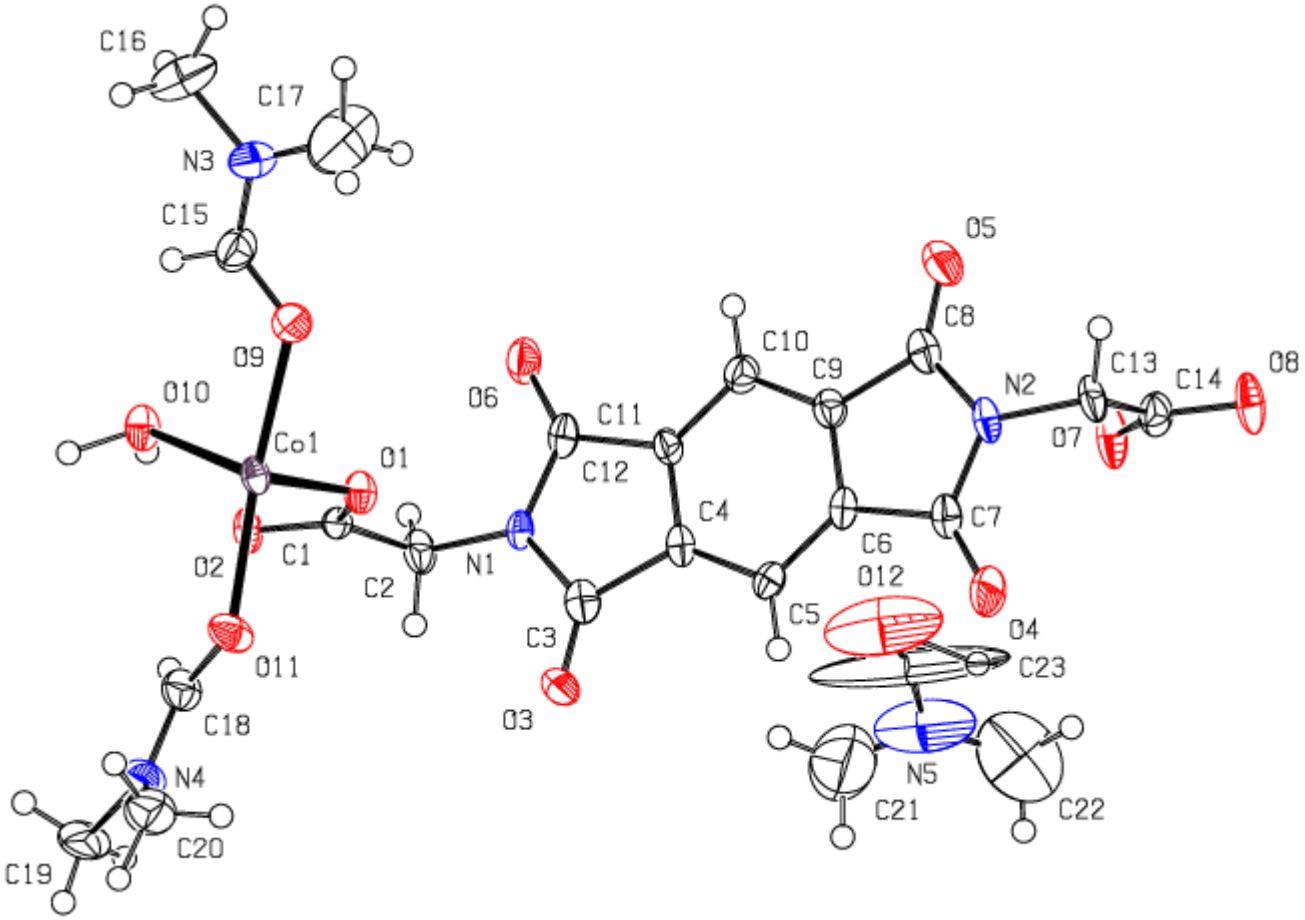

Figure 5.15: Ortep diagram of MOF-Co1 drawn at 50% probability level, indicating unresolved disorder in solvent DMF molecule.

5.5.4.1 Metal coordination

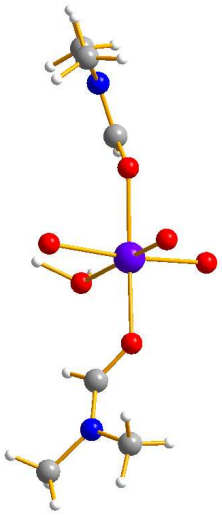

Figure 5.16: Coordination environment adopted by MOF-Co1.

An octahedral coordination environment is adopted by MOF-Co1. The coordination environment contains two DMF molecules attached at the apical positions, with a gly-L ligand and a water molecule coordinated to the equatorial plane. Just as with MOF-Zn1, the carboxylates coordinates differently to the metal. With one carboxylate group coordinating in a bridging bidentate fashion, whilst the other coordinated in a mondentate arrangement. The bridging arrangement occurs at an angle of 96.25^{o} (O1-Co-O2), and is responsible for the 2D extension of the structure. The adjacent apical DMF molecules associated with this structure indicates an offset arrangement with a torsion angle of 45.31^{o} (O9-Co1-Co1-O11).

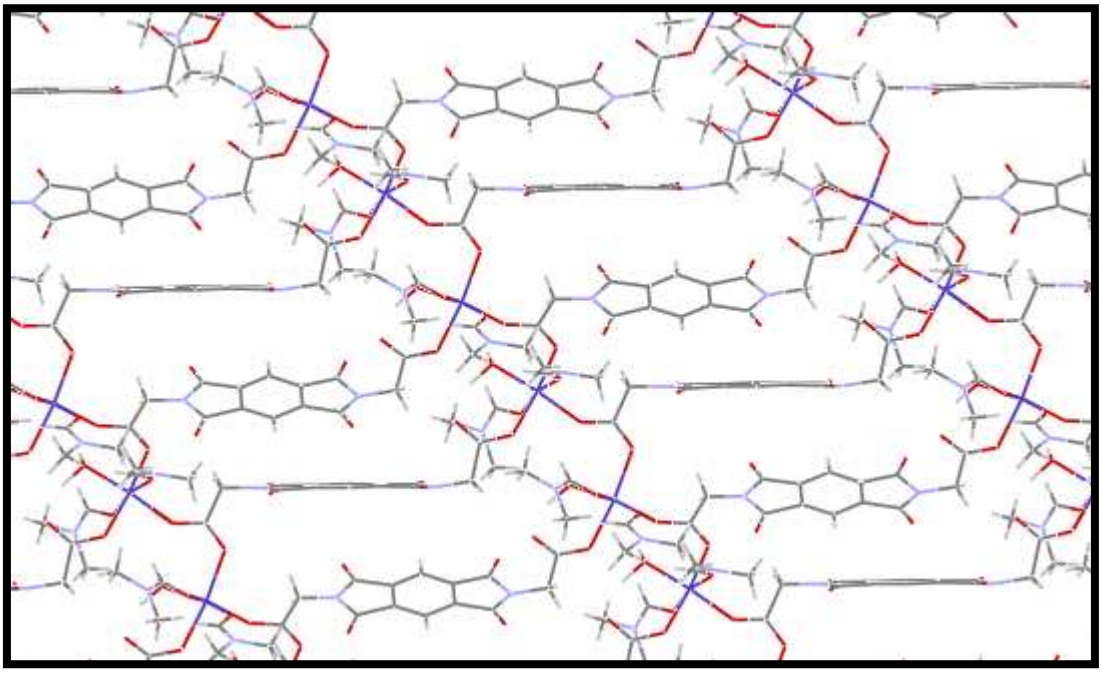

Figure 5.17: Offset two dimensional extension of MOF-Co1.

5.5.4.2 3D structure

The carboxylate bridging two metals, coupled with the ligand geometry and weak intermolecular hydrogen bonding allows for the step-like 2D extension of the structure, figure 5.17. The ligands components are arranged almost perpendicularly to each other and are offset by 82.70° (C5-H5-H10), with an inter-planar distance of 3.304Å, with alternate layers being aligned in a parallel manner. Three dimensional extension occurs only through weak intermolecular interactions between the planar IC carbonyls and the apical and solvent DMF molecules, table 5.5.

Table 5.5: CH···O hydrogen bonding interactions of MOF-Co1.

Molecular interaction	Interaction	D—H/Å	H···A/Å	D—H···A/Å	∟D—H···A/°
CH_2---GC (2D)	C13—Ha···O7	0.990	2.611	3.601(10)	131.61(30)
DMF---IC (3D)	C16—Hc···O6	0.980	2.471	3.451(13)	117.29(50)
DMF---IC (3D)	C22—Hb···O4	0.980	2.716	3.696(14)	145.66(70)

The removal of solvent molecules upon structure extension reveals the presence of 1D channels, again the removal of these molecules will lead to structure destabilization and collapse.

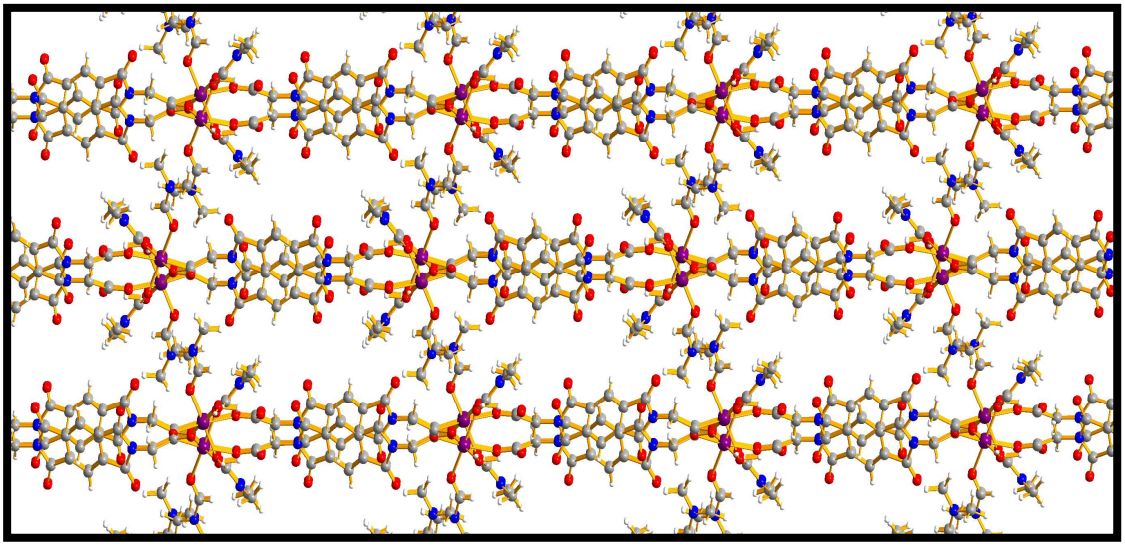

Figure 5.18: Pores in MOF-Co1 visible upon removal of solvent molecules as viewed down the *c*-axis.

5.6 PXRD DATA

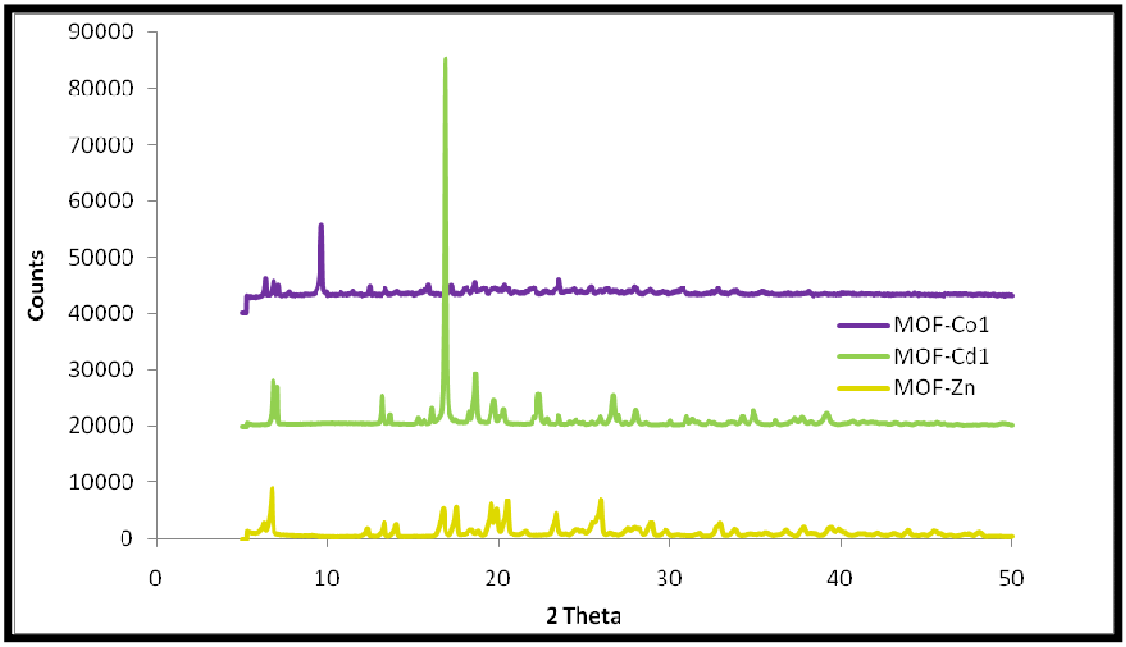

Figure 5.19: Experimental X-ray powder diffraction of MOF materials.

The observed PXRD patterns for all MOF materials do not align up with the expected powder patterns (appendix). A probable reason for this deviation from the expected patterns could be due to the evaporation of solvent molecules upon grinding, as well as a possible phase transitions of the material on cooling to -100^{o}C (SCXRD collection temperature) from room temperature (PXRD collection temperature). The large peak obtained in MOF-Cd1 is due preferred orientation.

5.7 Further experimental attempts to synthesise MOFs

Various synthetic methods were utilised at room temperature to aid in the formation of MOF materials. Methods included the use of different metal to ligand ratios (1:3, 1:2 and 1:1), as well as the use of blocking agents. It was however noted that none of these techniques had any effect on overall formation and the structure of the MOF material obtained.

Various thermal techniques were used also utilised on 1:2 and 1:3 metal to ligand ratios, these included high temperatures (120-140^{o}C) over short periods of time (6-10 hours). As well as medium temperature (80-100^{o}C) for longer periods (24-72 hours), different solvents were also used, as well as higher pressures in Teflon bomb reactors, but without success. Cooling techniques were also employed to slow down the rate of the reaction, but it did not yield any favourable results besides MOF-Co1.

The pillaring approach, as outlined by Chun *et al.* (2005) was also used in the formation of MOF materials. This method makes use of both dicarboxylates and diamine linkers in a one pot synthesis (Chun *et al*., 2005). They illustrated the use of the dicarboxylate linkers (L) was to form 2D layers, which could be then linked by the diamine linkers (P) to form 3D MOF materials (Chun *et al*., 2005). This approach did not yield any crystals. Synthesis attempts with different metal counterions in the form of acetates and chlorides were also made, but no promising results were obtained.

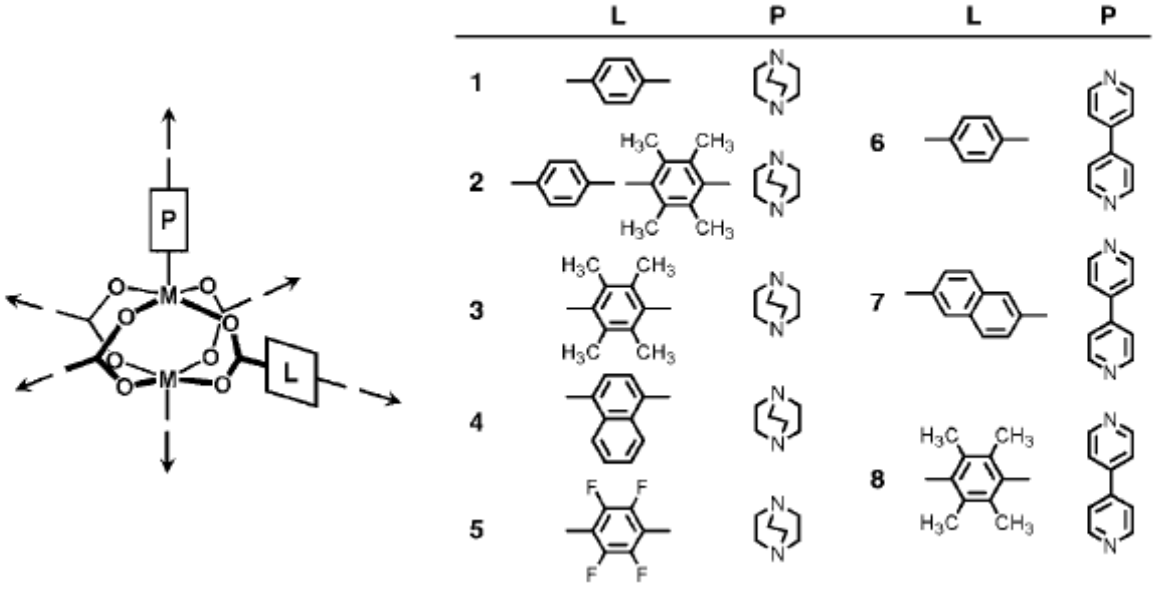

Figure: 5.20: Formation of 3D MOF using the pillaring approach (Chun *et al*., 2005).

Inclusion of cadmium ions into the MOF-Zn1 structure was also attempted. The synthetic method adopted for its formation was exactly the same as all other MOF structures and was carried out at room temperature. The main difference was attempted inclusion of cadmium metal in small amounts (10%) with zinc nitrate (90%). Optical microscopy indicated that this synthesis yielded MOF-Zn1 crystals exclusively.

The incorporation of aromatic rings within the framework was also attempted. This was done by placing the relevant amounts of donor (aromatic systems), host (ligand) and metal into a one pot synthesis. The crystallisation process led solely to the formation of CT complexes.

The but-L host molecule was also utilised as a linker component in the formation of novel MOF materials. Many of the techniques outlined above were employed, but unfortunately no MOF crystals could be grown by using but-L as a linker component.

5.8 Discussion

Metal organic frameworks are hybrid porous materials that can be modified by either changing the metal ion or the organic linker. Alterations of any one component can result in the formation of different topological frameworks, thereby changing the overall chemical and/or physical properties of the material. Within this project, four novel MOF materials were grown, using the gly-L ligand and three different divalent metal nitrates. SCXRD was successfully utilised to identifying the structural topology and bonding interactions of each MOF.

MOF-Zn was the only crystallisation that yielded two different crystals. All structures were obtained by utilising the vapour diffusion method at room temperature, except for MOF-Co1. The cobalt MOF required lower temperatures to crystallise as it showed a higher affinity toward gly-L than any other metal. All metals used in this study, adopted typical coordination environments for *d*-block metals. The adoption of

a trigonal-bipyramidal geometry by MOF-Zn1 proved to be somewhat surprising as this type of geometry is not commonly associated to d^{10} metals, while tetrahedral/octahedral environments are (Shriver *et al*,. 1999). However, it is believed that this type of coordination environment allows for the minimisation of ligand–ligand repulsion (Shriver *et al*,. 1999).

From each coordination environment, it was noted that all MOFs besides MOF-Zn2 contained solvent DMF molecules in the apical positions. All MOFs with a coordination number greater than 5 (trigonal bipyramidal and octahedral) contained a bridging ligand carboxylate group in the equatorial plane, which proved to be essential in the 2D extension of the structure. MOF-Co1 was the only structure to have a water molecule coordinated to it.

All structures extended in a similar fashion to gly-L with 2D and 3D extension occurring through the planar (IC) and terminal carbonyls (GC) groups. Solvent molecules within each structure played a vital role in the overall extension of the each respective framework. MOF-Zn1, Cd1 and Co1 extended via the bridging ligand to give 2D layers. The 2D sheets were then linked to each other through hydrogen bonding interactions between the apical DMF molecules to form 3D frameworks. Two dimensional extension of MOF-Zn1 leads to a herringbone formation, whereas MOF-Cd1 and Co1 yields step-like structures. MOF-Zn2 formed 1D chains through a centre of inversion, which extends into the third dimension through the solvent molecules that were present in the surrounding area. It was observed that the bonding characteristics and structural features of gly-L ligand component (figure 3.3) were retained within all the MOF frameworks. MOF-Zn2 and MOF-Cd1 were the only structures to form porous channels without the removal of solvent molecules.

Despite the formation of two porous structures, further inroads could not be made with regard to forming a sensor based MOF material. This was due to low porosity as well as poor crystal stability coupled with low yields for all MOF materials. This

made characterisation of these materials very difficult. Therefore further experimentation would be necessary to understand how these materials are formed under varying conditions, and how physical conditions affect the overall structure.

5.9 Reference

Chun, H., Dybtsev, D. N., Kim, H., Kim, K. (2005). Chem. Eur. J., 11, 3521.

Janiak, C. (2003). Dalton Trans, 14, 2781.

Kitagwa, S., Kitaura R., Noro S. (2004). Angew. Chem. Int. Ed., 43, 2334

Li, H., Eddaoudi, M., O' Keeffe, M., Yaghi, O. M. (1999). Nature. 402, 276.

Mueller U., Schubert M., Teich, F., Puetter, H., Schierle-Arndt K., Pastre, J. (2006). J. Mater. Chem., 16, 626

Shriver, D.F., Atkins, P. W. (1999). Inorganic Chemistry, 3rd edition, New York, Oxford, Oxford University Press, chapter 7.